

Sub-barrier Fusion of ${}^6\text{He}$ with ${}^{209}\text{Bi}$

J. J. Kolata,¹ V. Guimarães,¹ D. Peterson,¹ P. Santi,¹ R. White-Stevens,¹ P. A. DeYoung,² G. F. Peaslee,³ B. Hughey,² B. Atalla,² M. Kern,² P. L. Jolivet,² J. A. Zimmerman,⁵ M. Y. Lee,⁴ F. D. Becchetti,⁴ E. F. Aguilera,⁶ E. Martinez-Quiroz,⁶ and J. D. Hinnefeld⁷

¹*Physics Department, University of Notre Dame, Notre Dame, Indiana 46556*

²*Physics Department, Hope College, Holland, Michigan 49422*

³*Chemistry Department, Hope College, Holland, Michigan 49422*

⁴*Physics Department, University of Michigan, Ann Arbor, Michigan 48109*

⁵*Chemistry Department, University of Michigan, Ann Arbor, Michigan 48109*

⁶*Departamento del Acelerador, Instituto Nacional de Investigaciones Nucleares, A.P. 18-1027, C.P. 11801, Distrito Federal, Mexico*

⁷*Physics Department, Indiana University—South Bend, South Bend, Indiana 46615*

(Received 6 July 1998)

The fusion of ${}^6\text{He}$ with a ${}^{209}\text{Bi}$ target has been studied at energies near to and below the Coulomb barrier. Despite the weak binding of the valence neutrons in ${}^6\text{He}$, little evidence is found for suppression of fusion due to projectile breakup. Instead, a large enhancement of sub-barrier fusion is observed. It is suggested that this enhancement may arise from coupling to positive Q value neutron transfer channels, resulting in “neutron flow” between the projectile and the target. [S0031-9007(98)07674-1]

PACS numbers: 25.60.Pj, 25.70.Jj

Recent theoretical studies of near-barrier and sub-barrier fusion of the exotic “neutron halo” system ${}^{11}\text{Li}$ with ${}^{208}\text{Pb}$ (see, e.g., [1–5]) have generated a considerable amount of interest and controversy. The ${}^{11}\text{Li}$ nucleus contains two valence neutrons that are only very weakly coupled to a relatively tightly bound ${}^9\text{Li}$ core. This unusual composition manifests itself in both the structure of the nucleus, as in the existence of the neutron halo and of low-lying E1 modes [6], and also in reactions with other nuclei. Furthermore, neither the n - ${}^9\text{Li}$ nor the n - n subsystems of ${}^{11}\text{Li}$ are bound, so that particle stability in this nucleus is achieved via three-body interactions. Systems of this kind, referred to as “Borromean” nuclei [7], provide an unusual opportunity to study three-body interactions in the nucleus.

It has been known for some time that sub-barrier fusion of stable nuclei can be enhanced by several orders of magnitude beyond expectations from simple one-dimensional barrier penetration calculations. A qualitative understanding of this phenomenon has been achieved in terms of couplings to internal degrees of freedom of the target and projectile [8], resulting in a lowering of the effective fusion barrier. This dynamical effect is a very sensitive probe of the nuclear structure of the colliding partners. A lowering of the barrier, by 20% or more, is also a general feature in the results for ${}^{11}\text{Li} + {}^{208}\text{Pb}$ fusion presented in [1–5], but the leading effect that was calculated in this case is a static one, resulting from the larger radius of the ${}^{11}\text{Li}$ “halo” wave function which allows the attractive nuclear force to act at longer distances. However, additional dynamical enhancement was obtained from the coupling to the soft E1 mode [1,2]. The role played by projectile breakup channels, which are possibly important due to

the weak binding of the valence neutrons, is considerably more controversial. Several groups [2–4] have reported that coupling to these channels reduces the fusion cross section near the barrier, leading to intriguing structure in the excitation function in this region. However, this point of view has been criticized by Dasso and Vitturi [5] who suggest that it results from a misunderstanding of the nature of multidimensional quantum-mechanical tunneling processes. They report only enhancement of the fusion yield, even in the presence of strong breakup channels. It is important to resolve this controversy since the competition between projectile breakup and sub-barrier fusion enhancement will have important implications for attempts to form superheavy elements via fusion of exotic, neutron-rich projectiles [9].

The ${}^{11}\text{Li} + {}^{208}\text{Pb}$ system is at present inaccessible near the Coulomb barrier due to the low flux and poor energy resolution of ${}^{11}\text{Li}$ beams at these low energies. However, the ${}^6\text{He}$ nucleus, with two weakly bound neutrons around a ${}^4\text{He}$ core, has a “neutron-skin” structure [10] and might be expected to display some effects similar to those discussed above. It is also the simplest of the Borromean nuclei, and the fusion of its “core” with ${}^{209}\text{Bi}$ has been studied [11]. On the other hand, its two-neutron separation energy is 0.98 MeV (vs only 0.30 MeV for ${}^{11}\text{Li}$) so the wave function of its valence neutrons does not extend as far (hence, neutron “skin” rather than neutron “halo”) and breakup effects are probably less important. Unfortunately, fusion calculations for ${}^6\text{He}$ do not exist at present. In this work, we report on a measurement of near and sub-barrier fusion in the ${}^6\text{He} + {}^{209}\text{Bi}$ system which was undertaken in order to stimulate theoretical calculations of the various reaction and structure effects,

discussed above for the more complex ^{11}Li Borromean nucleus, in the context of the simpler ^6He case.

The ^6He beam used in this experiment was produced by *Twinsol*, a modified and upgraded version of a radioactive nuclear beam (RNB) facility that has been in operation at the University of Notre Dame since 1987 [12,13]. Two large superconducting solenoids act as thick lenses to collect and focus the secondary beam of interest into a 5 mm full width at half maximum (FWHM) spot [14]. For the purposes of this experiment, the most important feature of the upgrade was an increase in the maximum axial field integral from 1.5 to 3.9 T · m. This means that the energy of all secondary beams is now limited by the maximum primary beam energy from the accelerator rather than by the bending power of the solenoids. For example, a ^6He beam can be produced at energies up to 35 MeV, which is sufficient to study the fusion cross section of interest from below to well above the Coulomb barrier at about 20 MeV. In this case, the primary beam is ^7Li at an energy of 40 MeV, incident on a target consisting of a 12 μ foil of ^9Be . Primary beam currents of up to 200 particle · nA (pnA) are available. The secondary beam flux was calibrated by inserting a Si ΔE - E telescope at the secondary target position and reducing the intensity of the primary beam by 3 orders of magnitude so that the ^6He particles could be directly counted, while at the same time the primary beam current was measured in a Faraday cup. In this way, the ^6He production rate was determined to be 900 particles per second per pnA, and the maximum secondary beam intensity was $1.8 \times 10^5 \text{ s}^{-1}$.

This experiment was performed in an early implementation phase of the *Twinsol* project, and only one of the two solenoids was used. The function of the second solenoid is to purify the secondary beam, so the purity of the ^6He beam (determined using the telescope at the secondary target position) is potentially a concern. The main contaminant was ^3H with a rate similar to that of ^6He . However, detection of the fusion products was carried out via their characteristic delayed α -particle activities, so that ^3H -induced reactions cannot be confused with ^6He fusion. There was also a small ^4He contaminant, at an energy of 1.5 times that of the ^6He beam. This is far too high an energy to produce any ^{212}At via $1n$ evaporation [11]. Incomplete fusion of the ^4He core, followed by $1n$ emission to ^{212}At , is also not a concern due to the $-19 \text{ MeV } Q$ value for this reaction channel.

PACE calculations [15] indicate that the ^{215}At compound nucleus decays exclusively by the evaporation of 2, 3, or 4 neutrons when formed via $^6\text{He} + ^{209}\text{Bi}$ fusion at the beam energies used in the present experiment. The $4n$ channel has been measured in a previous work [16], and shown to be well described by PACE. The effect of the $2n$ channel is small except at energies well below the barrier. Thus, the total fusion cross section deduced from this work may somewhat underestimate the actual yield at the lowest measured energies.

The new data presented here are the result of a measurement of the $3n$ -emission channel, which dominates in the vicinity of the Coulomb barrier. The ^{212}At evaporation residue can be formed in its 1^- ground state, which decays with a half-life of 314 ms by the emission of two closely spaced α groups with an average energy of 7662 keV, or in the 9^- isomeric state which decays with a half-life of 119 ms, again by the emission of two closely spaced α groups in this case having an average energy of 7848 keV [17]. The delayed α particles were detected in a “box” consisting of four large-area (3 cm × 3 cm) Si detectors placed directly behind the target. The efficiency of this arrangement was found to be $21 \pm 1\%$ using a calibrated source, in agreement with a Monte Carlo simulation. The energy resolution of the detectors, approximately 100 keV FWHM, was insufficient to resolve the closely spaced groups mentioned above (which have a separation of 60 keV), and the ability to separate the ground-state from the isomeric-state decay on the basis of average α -particle energy alone was marginal, but identification of the $3n$ evaporation product was unambiguous. In order to eliminate the background coming from prompt reactions, the primary beam was pulsed using several different irradiate/count protocols in order to allow for the determination of the isomer ratio in the production of ^{212}At . The majority of the data were taken with a “beam on” period of 0.3 s and counting periods of either 0.3 or 0.6 s (separated by “transition” periods of 10 ms), and the time of each event relative to the beginning of a counting cycle was recorded. Primary beam energies of 32, 35, and 37 MeV were used. Absorbers of 8, 16, or 24 μm Havar foil were placed in front of the 1 mg/cm 2 Bi target, which was 2.5 cm in diameter, in order to provide finer energy steps, and repeat points with different absorber and primary beam energies were taken to ensure consistency. The results are shown in Fig. 1, compared with a PACE calculation. It can be seen that the

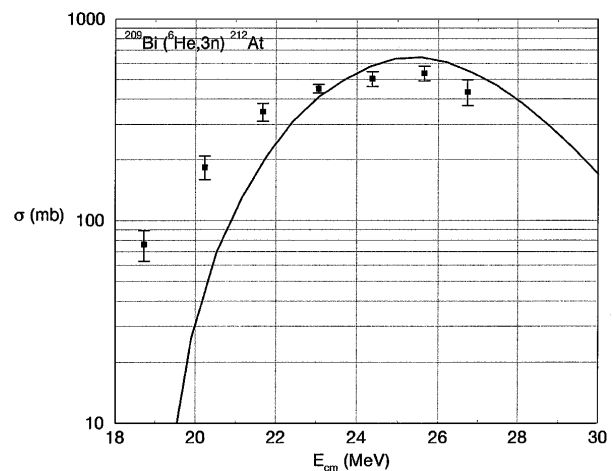


FIG. 1. Excitation function for the $^{209}\text{Bi} (^6\text{He}, 3n)$ reaction. The solid curve is a PACE calculation.

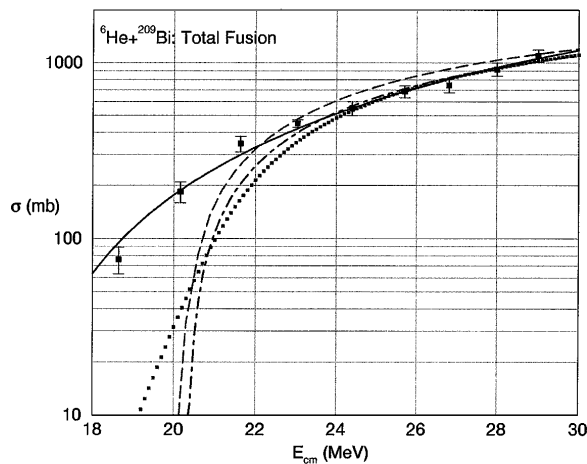


FIG. 2. Total cross section for ${}^6\text{He} + {}^{209}\text{Bi}$ fusion. The dashed curve is the PACE prediction for the total fusion cross section, the dotted curve is a CCFUS calculation, and the dot-dashed curve is the result of a linear least-squares fit to the high-energy data on a $1/E_{\text{c.m.}}$ plot (see text). The solid curve is explained in the text.

agreement at above-barrier energies is very good. However, there is an increasing discrepancy at lower energies, signaling sub-barrier fusion enhancement.

The total fusion cross section, obtained by adding the $3n$ and $4n$ yields, is compared with several calculations in Fig. 2. Note that the center-of-mass (cm) energies at which the data points are displayed have been corrected for the finite energy resolution of the secondary beam by folding the excitation function (solid curve) with a Gaussian of 1.5 MeV FWHM and using the result to determine the actual average cm energy. This procedure was iterated until a self-consistent result was obtained. The highest-energy points were then fit to a straight line on a $1/E_{\text{c.m.}}$ plot to determine the fusion barrier height and radius (see, e.g., [18]). The results are compared with systematics, and with parameters determined (by us) from the ${}^4\text{He} + {}^{209}\text{Bi}$ data, in Table I. The PACE prediction for the total fusion cross section (including the $2n$ channel) is the dashed curve in Fig. 2; a similar calculation for ${}^4\text{He} + {}^{209}\text{Bi}$ fusion provides a very good fit to the experimental data of Ref. [11]. The dotted curve is an uncoupled (i.e., pure barrier penetration) calculation using the code CCFUS [19]. The dot-dashed curve was obtained using the experimental barrier and radius parameters from this work given in Table I. The barrier is shifted by about -0.7 MeV relative to ${}^4\text{He}$ -induced fusion, in approximate agreement with the PACE estimates but less than that from

the Gupta and Kailas systematics [18]. This relatively small shift is expected for the “neutron-skin” nucleus ${}^6\text{He}$, since the valence neutron wave function does not extend to very large radii as in ${}^{11}\text{Li}$. The radius parameter R_b is smaller than the PACE estimate, possibly suggesting fusion suppression in the barrier region of about 6% (comparable to the estimated 10% uncertainty in the absolute cross section), or 20% if the parameters from [18] are used. Either result is very much smaller than the effect computed for ${}^{11}\text{Li}$ in [2–4], and there is no sign of the predicted structure in the fusion excitation function due to projectile breakup. On the other hand, the neutron binding energies are larger for ${}^6\text{He}$ than for ${}^{11}\text{Li}$, and it is also possible that structure might occur at energies below that measured in this experiment. Detailed theoretical calculations are necessary to address these issues, but we conclude that there is little evidence in the present data set for fusion suppression due to projectile breakup, in agreement with the results of Yoshida *et al.* [20] for the ${}^{11}\text{Be} + {}^{209}\text{Bi}$ system.

There is, however, a very clear signature for sub-barrier enhancement of fusion relative to the one-dimensional barrier penetration calculations in Fig. 2. A particularly enlightening way to present the data in this case has been introduced by Stelson *et al.* [21], who noted that many fusion excitation functions near the barrier have the property that $(E_{\text{c.m.}}\sigma)^{1/2}$ is linear, even in the presence of large enhancements relative to potential-model estimates. They further show that this behavior results from the introduction of a distribution of barriers with uniform weight extending from some threshold energy T to $2B-T$, where B is the nominal barrier. Such a plot is shown in Fig. 3 for the present data set. It is clear that all points follow a linear trend, and we deduce a barrier shift $B-T$ of 5.14 ± 0.08 MeV and a threshold energy T of 15.4 ± 0.2 MeV, implying a 25% dynamical reduction in the barrier height. (The excitation function corresponding to this parametrization, shown as the solid curve in Fig. 2, provides an excellent fit to the data.) Dynamical coupling to the soft E1 mode has been included [1,2] in the existing sub-barrier fusion calculations for ${}^{11}\text{Li}$. However, Stelson *et al.* noticed that the threshold barrier T correlates with neutron binding energies (not collective properties of the participating nuclei), as would be expected if the fusion cross section in the near sub-barrier region reflects neck formation promoted by “neutron flow” [21]. In the context of the coupled-channels approach, neutron flow is enhanced by the availability of strong,

TABLE I. Comparison of fusion barrier heights (MeV) and radii (fm).

Reference	$V_b({}^6\text{He})$	$V_b({}^4\text{He})$	$R_b({}^6\text{He})$	$R_b({}^4\text{He})$
This work	20.3 ± 0.2	20.98 ± 0.05	10.40 ± 0.04	10.04 ± 0.01
PACE	20.02	20.80	10.74	10.00
Ref. [18]	19.76	20.96	11.56	10.68

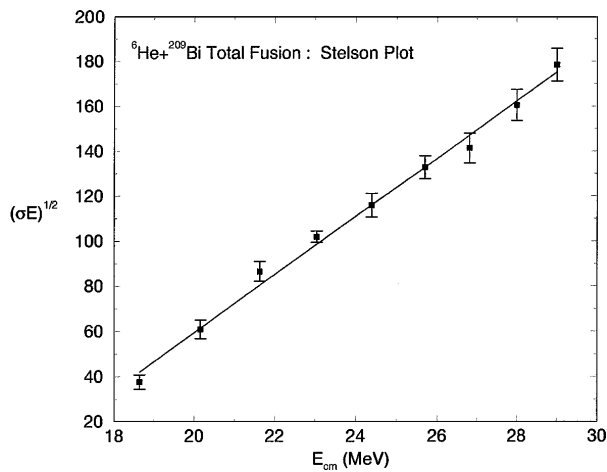


FIG. 3. Stelson plot for the total fusion data; the curve is a linear least-squares fit. The two highest-energy points in this and the previous figure were obtained by adding an estimate of the $3n$ cross section (see Fig. 1) to the dominant $4n$ yield from Ref. [16]. See text for further discussion.

positive Q -value neutron transfer channels [22]. This is just the situation for ${}^6\text{He} + {}^{209}\text{Bi}$, where the one- and two-neutron transfer channels have Q values of +2.7 and +8.8 MeV, respectively, compared with the ${}^4\text{He}$ case where the corresponding Q values are all large and negative. It would appear, therefore, that neck formation via neutron flow is an excellent candidate to explain the observed large sub-barrier fusion enhancement.

In summary, we have for the first time studied near-barrier and sub-barrier fusion of an exotic “Borromean” nucleus. Despite the weak binding of the valence neutrons in ${}^6\text{He}$, little evidence was found for suppression of fusion due to projectile breakup. On the contrary, we find only a large enhancement of sub-barrier fusion, implying a striking 25% reduction in the nominal fusion barrier. Arguments were given to suggest that the observed enhancement may result from coupling to positive Q value neutron transfer channels, leading to “neutron flow” and consequent neck formation between the projectile and the target. Surprisingly, this effect has apparently been neglected in all existing calculations of ${}^{11}\text{Li} + {}^{208}\text{Pb}$ fusion, despite the presence of weakly bound valence neutrons and many positive Q value neutron transfer channels (including in this case the transfer of neutrons from the ${}^9\text{Li}$ core). Detailed theoretical calculations are urgently needed to test this speculation.

Support for this work was provided by the U.S. National Science Foundation (NSF) under Grants No. PHY94-02761 (Notre Dame), No. PHY95-12104 (Michigan), and No. PHY98-70262 (Hope College). The Twinsol construction project was funded by the NSF under Academic Research Instrumentation Grant No. PHY95-12199. The Mexican group is supported by a grant from CONACYT (Mexico). One of us (V.G.) was supported by the FAPESP (Brazil) while on leave from the Universidade Paulista.

- [1] C. Dasso, J.L. Guisardo, S.M. Lenzi, and A. Vitturi, *Nucl. Phys.* **A597**, 473 (1996).
- [2] N. Takigawa, M. Kuratani, and H. Sagawa, *Phys. Rev. C* **47**, R2470 (1993).
- [3] M.S. Hussein, M.P. Pato, L.F. Canto, and R. Donangelo, *Phys. Rev. C* **46**, 377 (1992); **47**, 2398 (1993).
- [4] M.S. Hussein, *Nucl. Phys.* **A588**, 85c (1995).
- [5] C. Dasso and A. Vitturi, *Phys. Rev. C* **50**, R12 (1994).
- [6] K. Ieki *et al.*, *Phys. Rev. Lett.* **70**, 730 (1993).
- [7] M.V. Zhukov, B.V. Danilin, D.V. Federov, J.M. Bang, I.J. Thompson, and J.S. Vaagen, *Phys. Rep.* **231**, 151 (1993).
- [8] M. Beckerman, *Rep. Prog. Phys.* **51**, 1047 (1988).
- [9] S. Hofman, *Rep. Prog. Phys.* **61**, 639 (1998).
- [10] I. Tanihata *et al.*, *Phys. Lett. B* **289**, 261 (1992).
- [11] W.J. Ramler, J. Wing, D.J. Henderson, and J.R. Huizenga, *Phys. Rev.* **114**, 154 (1959).
- [12] J.J. Kolata, A. Morsad, X.J. Kong, R.E. Warner, F.D. Becchetti, W.Z. Liu, D.A. Roberts, and J.W. Jänecke, *Nucl. Instrum. Methods Phys. Res. Sect. B* **40/41**, 503 (1989).
- [13] F.D. Becchetti and J.J. Kolata, in *Application of Accelerators in Research and Industry*, edited by J.L. Duggan and I.L. Morgan, AIP Conf. Proc. No. 392 (AIP Press, New York, 1997), pp. 369–375.
- [14] M.Y. Lee, *et al.*, in *Application of Accelerators in Research and Industry* (Ref. [13]), pp. 397–400.
- [15] A. Gavron, *Phys. Rev. C* **21**, 230 (1980).
- [16] P.A. DeYoung *et al.*, *Phys. Rev. C* (to be published).
- [17] *Table of Isotopes*, edited by R.B. Firestone and V.S. Shirley (Wiley, New York, 1996), 8th ed.
- [18] S.K. Gupta and S. Kailas, *Phys. Rev. C* **26**, 747 (1982).
- [19] J. Fernandez-Niello, C.H. Dasso, and S. Landowne, *Comput. Phys. Commun.* **54**, 409 (1989).
- [20] A. Yoshida *et al.*, *Phys. Lett. B* **389**, 457 (1996).
- [21] P.H. Stelson, H. Kim, M. Beckerman, D. Shapira, and R.L. Robinson, *Phys. Rev. C* **41**, 1584 (1990).
- [22] H. Timmers *et al.*, *Phys. Lett. B* **399**, 35 (1997).